ACS APPLIED MATERIALS & INTERFACES

Research Article

www.acsami.org

Isolation of Viable Type I and II Methanotrophs Using Cell-Imprinted Polyurethane Thin Films

Yufeng Hu, Lin Xie, Yahai Lu, and Xueqin Ren*

Department of Environmental Sciences & Engineering, College of Resources and Environmental Sciences, China Agricultural University, Beijing, People's Republic of China, 100193

Supporting Information

ABSTRACT: Studies on methanotrophs utilizing methane as sole source of carbon and energy are meaningful for governing global warming; although, the isolation of methanotrophs from nature is challenging. Here, surface imprinted polyurethane films were fabricated to selectively capture living methanotrophs from paddy soil. Two tracks of molecularly imprinted film based on polyurethane (PU-MIF$_1$ and PU-MIF$_2$) were imprinted using type I or II methanotrophs as template, respectively, and then reacted with polyethylene glycol, castor oil, and hexamethylene diisocyanate. Results demonstrated these PU-MIFs hold low water absorption rate and superior biocompatibility, which was highly demanded for maintaining cell viability. Superior selectivity and affinity of PU-MIFs toward their cognate methanotroph cells was observed by fluorescent microscopy. Atomic force microscopy revealed the adhesion force of PU-MIFs with its cognate cells was much stronger in comparison with noncognate ones. Using the as-prepared PU-MIFs, within 30 min, methanotroph cells could be separated from rice paddy efficiently. Therefore, the PU-MIFs might be used as an efficient approach for cell sorting from environmental samples.

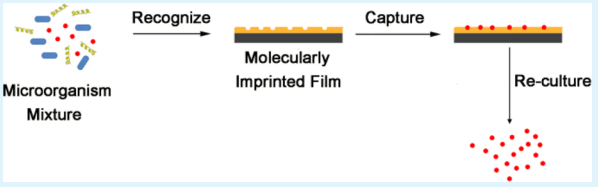

KEYWORDS: *cell isolation, methanotroph, molecularly imprinted film, polyurethane, viability*

1. INTRODUCTION

Methane is the second most important greenhouse gas because it is responsible for about one-fifth of the global warming induced by long-lived greenhouse gases since 1750, and its atmospheric concentration has been rising again recently.[1] The main emission of methane comes from the biogenic sources of natural wetlands and rice paddies.[2] Studies have proved that methanotrophs are a group of Gram-negative bacteria utilizing methane as their sole source of carbon and energy.[3] And more than 90% of the methane produced in the anaerobic environments of rice paddies can be oxidized by methanotrophs in the aerobic zones.[4] Due to the oxidation by methanotrophs, the actual amount of methane emitted from wetland and rice paddies to atmosphere is reduced substantially.[3] Thus, many studies have been carried out to understand the diversity and functioning of methanotrophs in the environment. Unfortunately, the isolation of the uncharacterized methanotrophs from environmental samples has been difficult due to the low selectivity and time-consuming approaches of traditional enrichment methods.[5]

Molecularly imprinted polymers (MIPs) for small molecules are formed in the presence of template molecules, which are removed afterward leaving complementary cavities, and thus, the MIPs possess highly specific affinity for target molecules.[6−9] To our knowledge, reports for imprinting microorganisms have still been rare. Dickert and co-workers have developed a kind of molecularly imprinted polyurethane film to selectively detect yeast cell.[10−12] Subsequently, Hachulka et al. applied MIP-based polyacrylate to selectively adsorb *Saccharomyces cerevisiae* cells and quantitatively measured the adhesion forces between *S. cerevisiae* cells and MIPs.[13] In 2012, Schirhagl et al. adopted MIPs combined with microfluidic device to separate cyanobacteria from the mixture of two strains of cyanobacteria.[14] Following this method, Ren and co-workers sorted inactivated *Mycobacterium smegmatis* cells from the mixture composed of three known microorganisms.[15] Nonetheless, due to the complexity of real samples, difficulties in obtaining template cells, and the limited lifetime of live target cells, living cell separation from real samples is still a great challenge.

Here, we developed a previously undescribed method to separate living methanotrophs from rice paddies by introducing type I and II methanotroph cells into polyurethane-based molecularly imprinted films (PU-MIF), which were named PU-MIF$_1$ and PU-MIF$_2$, respectively. To enhance the applicability of PU-MIFs in living cell separation, we used poly(ethylene glycol),[16] castor oil, a kind of vegetable oil,[17] and 1,6-hexamethylene diisocyanate to prepare superior biocompatible PU-MIFs. The PU-MIFs were evaluated by water absorption rate and biocompatibility first. And then selective recognition of PU-MIFs toward their template methanotrophs was visually characterized by fluorescent microscopy. To quantitatively investigate the affinity of methanotroph toward different PU-MIFs surface, the adhesion forces between methanotrophs and PU-MIFs were measured by atomic force microscopy (AFM)

Received: September 11, 2014
Accepted: October 31, 2014
Published: October 31, 2014

in force spectroscopy mode. Finally, the PU-MIFs were applied into the separation of methanotrophs from real rice paddies.

2. EXPERIMENTAL SECTION

2.1. Materials. Poly(ethylene glycol) (PEG; M_w, 400), castor oil (CO), 1,6-hexamethylene diisocyanate (HDI), and 3-aminopropyltriethoxysilane (APTES) were purchased from Sigma (St. Louis, MO). *Methylomicrobium album* (ATCC 33003, type I methanotroph, type strain) and *Methylosinus trichosporium* (ATCC 49242, type II methanotroph, type strain) were obtained from ATCC (Manassas, VA). CellTracker Orange CMTMR (C2927) and CellTracker Green CMFDA (C2925) were purchased from Invitrogen (Carlsbad, CA). Trimethyl chlorosilane (TMCS) and dimethyl sulfoxide (DMSO, ultrapure) were obtained from J&K (Beijing, China). Phosphate-buffered saline (PBS, pH 7.2−7.4) was purchased from Beijing Tuoyingfang Biotech Co., Ltd. (Beijing, China). Silicon nitride cantilever (MLCT-C, spring constant was 0.03 N/m) was obtained from Bruker, and was purchased from Veeco (New York).

2.2. Culture of Methanotroph Type Strains and Isolation of Methanotroph from Paddy Soil. Two type strains of methanotroph (ATCC 33003 and ATCC 49242) were chosen as the template for PU-MIFs preparation. We followed the culturing protocol for these two types of methanotroph according to the manufacturer's instructions for ATCC 49242. Briefly, ATCC medium 1057 was prepared for transforming ATCC 33003 from vial into broth tube, while ATCC medium 1683 was prepared for ATCC 49242. Then, 0.5 mL of the above mixtures was placed into another broth tube containing 5 mL of each corresponding medium. Subsequently, both cultures were incubated at 25 °C with a gas mixture of 50% methane−50% air. After three generations, the cultured methanotroph was used for experiments.

The paddy soil used for methanotroph separation by PU-MIFs was collected from a rice field at China National Rice Research Institute in Hangzhou, China. Paddy soil (4 g) was placed into a 100 mL culture bottle with cap, and then 11 mL of potassium nitrate solution was added (200 mg potassium nitrate/kg soil). Pure methane was purged into the above sample, and the final methane concentration at 13%. Then the sample was incubated at 25 °C with continuous rotation at 250 rpm. At 8, 16, 24, and 32 days, the potassium nitrate was replenished. During the cultivation, gas chromatography was used to monitor the concentration of methane in the culture bottle. Once the methane concentration in the culture bottle dropped to around 100 ppm, the gas in the culture bottle needed to be replaced with sterilized fresh gas with a methane concentration of 13% to maintain the activity of methanotroph. After 39 days of incubation, 1 mL of slurry was injected into the fresh sterilized culture solution (same components with type methanotroph) for methanotroph isolation by PU-MIFs.

2.3. Preparation of Template Stamps and Fabrication of PU-MIFs. A prerequisite for imprinting with methanotroph cell is a glass stamp with adhered cells. For this purpose, 10 μL of fresh cell suspension was spread out on a precleaned microscope slides. After incubation for 30 min at 4 °C, the surplus solvent was removed by spinning the slide at 4000 rpm using VTC-100 spin-coater (MTI, Shenyang, China) prior to drying. And the stamps with adhered methanotroph cells were obtained.

Prior to the synthesis, PEG was dried with continuous stirring under vacuum at 90 °C for 2 h, and CO was dried by a similar method at 105 °C. Polyurethane (PU) film was synthesized using a two-step bulk polymerization with a 1:2.3:1 molar ratio of PEG/HDI/CO. First, HDI was reacted with PEG at 80 °C for 4 h with vigorous stirring in a 250 mL three-neck flask at normal pressure, and then the mixture was reacted with CO at 80 °C for 30 min. A thin-layer PU film was obtained by casting the mixture on silicon wafer by spin-coater. Then, stamps with adhered methanotroph cells were pressed against the PU film, and the PU film was cured and aged at 25 °C in a vacuum oven for 24 h. Then, the stamp was peeled off, and the parts of methanotroph cells used for the production of imprinted sites were taken away from the PU film at the same time. To remove the residual methanotroph cells, the remaining film was sonicated in hot water for 10 min. The final PU-MIFs were obtained after being dried at 60 °C in vacuum oven for 24 h. Simultaneously, polyurethane nonimprinted film (NIF) was produced using the same procedure without templates.

2.4. SEM and AFM. The surface morphology of PU-MIFs and NIF was observed by SEM (S-4800, Hitachi Science System, Japan) with an accelerating voltage of 20 kV. Prior to observation, samples were coated with gold with a thickness of 2−3 nm using a coating system (JFC-1600 Auto Fine Coater, JEOL, Tokyo, Japan).

To study the adhesive properties of PU-MIFs and NIF, we applied the AFM technique in force spectroscopy mode. All adhesion force measurements were performed on an AFM (Asylum Research, Santa Barbara, CA) in liquid conditions, that is, buffer for the culture of ATCC 33003 and ATCC 49242. Methanotroph type strains of ATCC 33003 and ATCC 49242 were separately stuck at the end of the AFM cantilever, which was previously salinized according to the protocol of Blanchette's research.[18] Prior to the adhesion measurements, the spring constants of both cantilevers immobilized with cells were calibrated, and the obtained values were 39.29 pN/nm for ATCC 33003 and 40.44 pN/nm for ATCC 49242. The force curves were recorded over the scanned area of 400 μm^2 with 100 force points measured. Data treatment referred to the former publication.[19]

2.5. Measurement of Water Absorption Rate. PU-MIFs or NIF with same weight was immersed into distilled water at room temperature. After 0.5, 1.0, 1.5, 2.0, 2.5 and 4.0 h, the weights of polymers were weighed after water residue on the polymer surfaces was wiped off with paper towel. The water absorption rate (WAR) of polymers was calculated using the equation $WAR = (W_t - W_0)/W_0$, where W_0 and W_t are polymer weights before and after water absorption.

2.6. Evaluation of Biocompatibility. To further study the application probability, we investigated the biocompatibility of PU-MIFs using both methanotroph type strains and methanotroph mixture extracted from paddy soil. For methanotroph type strains, light microscopy was used to compare the shape and size of methanotrophs. Sterilized PU-MIFs with same weight were immersed into the culture solution, and aliquots of cultured methanotrophs were added. Simultaneously, a control methanotroph culture solution (i.e., without PU-MIFs) was also prepared. After 72 h, part of the methanotroph solution cultured with or without PU-MIFs was harvested and observed under light microscopy.

For microorganism mixtures extracted from paddy soil, OD_{600} and CH_4 consumption were carried out for further justification. First, methanotroph mixtures with or without sterilized PU-MIFs were incubated under the same conditions. Then, the OD_{600} value of the sample was obtained by UV spectroscopy analysis, and simultaneously, the CH_4 amount in sample was detected by gas chromatography (GC; Shanghai Precision and Scientific Instrument, Shanghai, China). The CH_4 consumption amount was obtained by subtracting the remaining CH_4 amount from the initial CH_4 after incubation.

2.7. Methanotroph Sorting and Characterizations. For sorting of methanotroph type strains, fluorescence microscopy was used to observe the separation efficiency. The freshly cultured type I methanotroph (ATCC 33003) and type II methanotroph (ATCC 49242) were stained with CellTracker Green CMFDA and CellTracker Orange CMTMR, respectively, according to the manufacturer's instructions. These two kinds of stained cells were resuspended using 15 mL of PBS and subpackaged into 6 aliquots. Then, sterilized PU-MIF_1, PU-MIF_2, and NIF were separately added into one of the stained ATCC 33003 or ATCC 49242 solutions. After 2 h of incubation, PU-MIF_1, PU-MIF_2, and NIF were taken out and washed by PBS five times to remove fluorescent dye residue. Subsequently, PU-MIF_1, PU-MIF_2, and NIF were observed by an Olympus FV1000 Confocal Laser Scanning Microscope (Tokyo, Japan). The excitation wavelength for CellTracker Green CMFDA and CellTracker Orange CMTMR were set at 488 and 543 nm, respectively.

The procedure of methanotrophs isolation from rice paddies was as follows. Sterilized PU-MIF_1, PU-MIF_2, and NIF were immersed into corresponding cultured microorganism mixture extracted from paddy soil. After incubation for 0.5 h, PU-MIF_1, PU-MIF_2, and NIF were

Scheme 1. Illustrations the Fabrication and Cell Capture of PU-MIFs: (a) Chemical Structures of Monomers Used for PU-MIF Fabrication, (b) Fabrication of PU-MIF, and (c) Re-Recognition of Template Cells

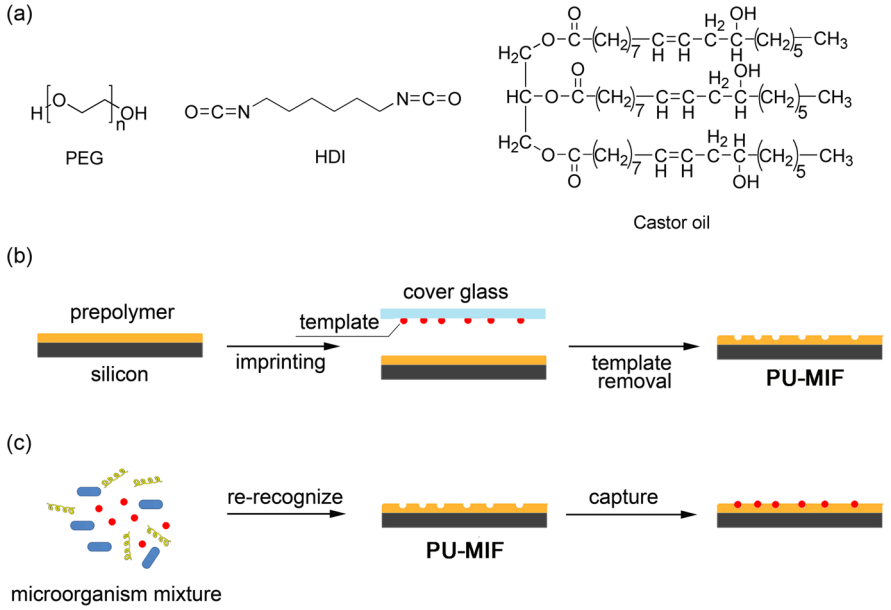

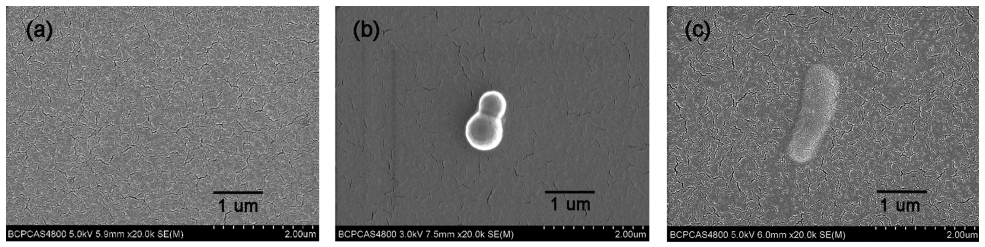

Figure 1. SEM images of (a) NIF, (b) PU-MIF$_1$, and (c) PU-MIF$_2$ after template removal.

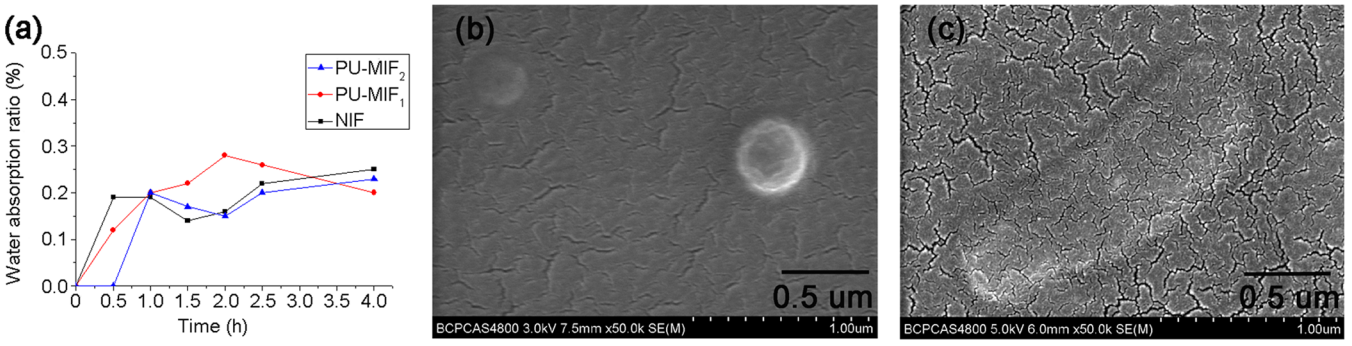

Figure 2. (a) Kinetic curves of the water absorption rate of PU-MIF$_1$, PU-MIF$_2$, and NIF. SEM images of cavities (b) PU-MIF$_1$ and (c) PU-MIF$_2$ after 4.0 h of water incubation.

picked up and washed by sterilized distilled water 10 times. Subsequently, the above PU-MIF$_1$, PU-MIF$_2$, and NIF samples were placed into fresh-cultured solutions to further incubate the adsorbed methanotrophs. The OD_{600} and CH_4 consumption amounts of the samples were monitored in real-time.

3. RESULTS AND DISCUSSION

3.1. Preparation and Characterization of PU-MIFs. In nature, there were mainly two kinds of methanotrophs carrying different physiological behaviors, namely type I methanotroph (*Methylomonas*, *Methylomicrobium*, *Methylobacter*, *Methylocaldum*, and *Methylosphaera*) and type II methanotroph (*Methylocystis* and *Methylosinus*).[20] The shape of type I methanotroph (ATCC 33003) and type II methanotroph (ATCC 49242) were cocco-bacilli and rod, respectively. To sort methanotrophs from real samples, two types of methanotroph were chosen as templates to prepare MIFs in our experiments. Scheme 1 illustrates the process flow of experiment, and two series of PU-MIFs (PU-MIF$_1$ and PU-MIF$_2$) were fabricated.

To validate the successful establishment of the imprinting sites, we examined surface morphologies of PU-MIF$_1$, PU-MIF$_2$, and NIF by SEM and AFM. For the surfaces of PU-MIF$_1$ (Figure S1a in Supporting Information) and PU-MIF$_2$ (Figure S1b in Supporting Information) without template removal, there were lots of cells on them, suggesting the successful

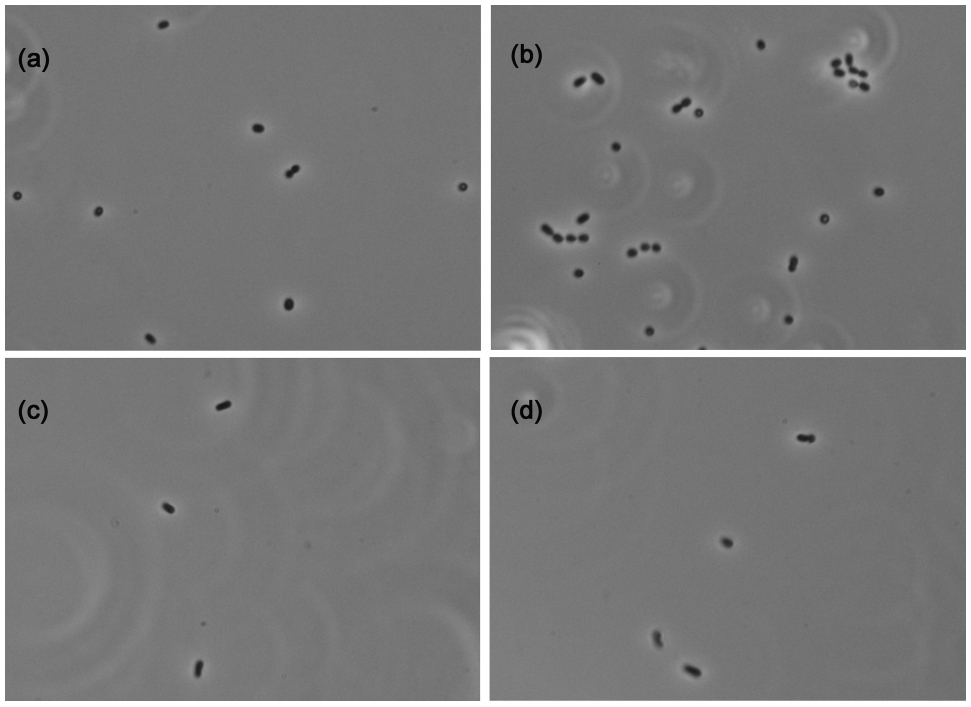

Figure 3. Bright field images of ATCC 33003 cultured (a) without PU-MIF$_1$ and (b) with PU-MIF$_1$ and of ATCC 49242 cultured (c) without PU-MIF$_2$ and (d) with PU-MIF$_2$.

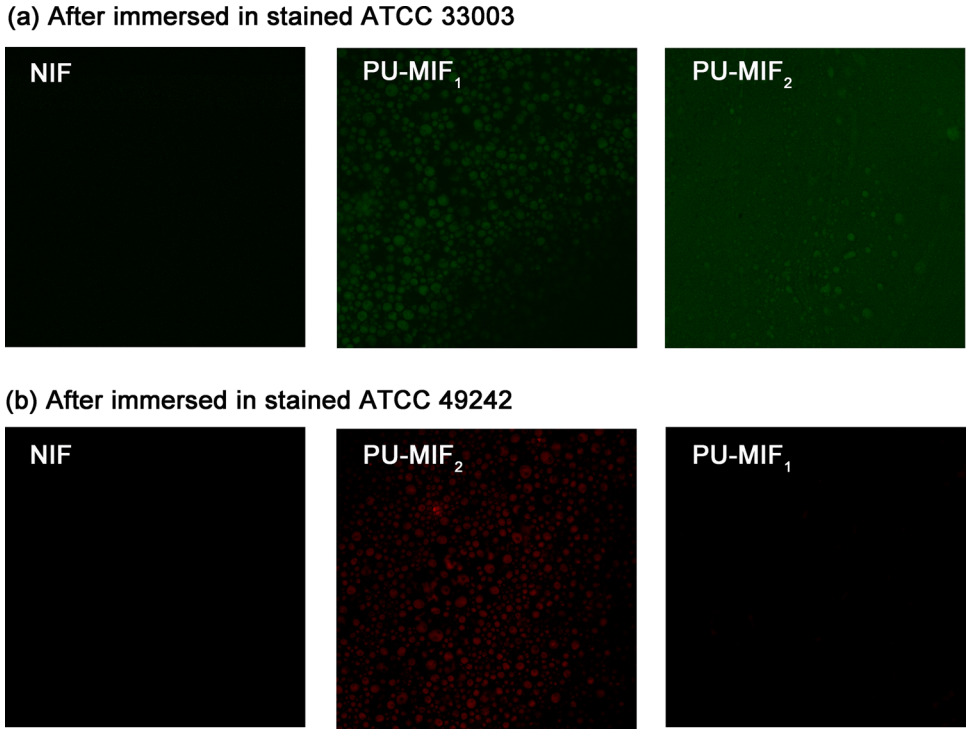

Figure 4. Fluorescent micrographs of PU-MIF$_1$, PU-MIF$_2$, or NIF preimmersed in (a) ATCC 33003 and (b) ATCC 49242. ATCC 33003 and ATCC 49242 were stained with CellTracker Green CMFDA and CellTracker Orange CMTMR, respectively.

introduction of the template cells. After the removal of template cells, cavities were produced on the surface of PU-MIF$_1$ and PU-MIF$_2$ (Figure 1b,c and Figure S2b,c in Supporting Information). And the sizes of the cavities were consistent with the original dimensions of the two methanotroph type strains, whereas the surface of NIF was very smooth and uniform (Figure 1a, Figure S2a in Supporting Information).

It was known that polyurethane polymer containing PEG was apt to swell in a water-abundant environment.[16,21] To ensure the integrity of the imprinted sites on the surface of PU-MIFs, swelling of the polymer should be minimized by optimizing the ratio among PEG, CO, and HDI. The water absorption rates of the PU-MIFs and NIF synthesized under optimal reaction condition were measured and remained very low (below 0.3%,

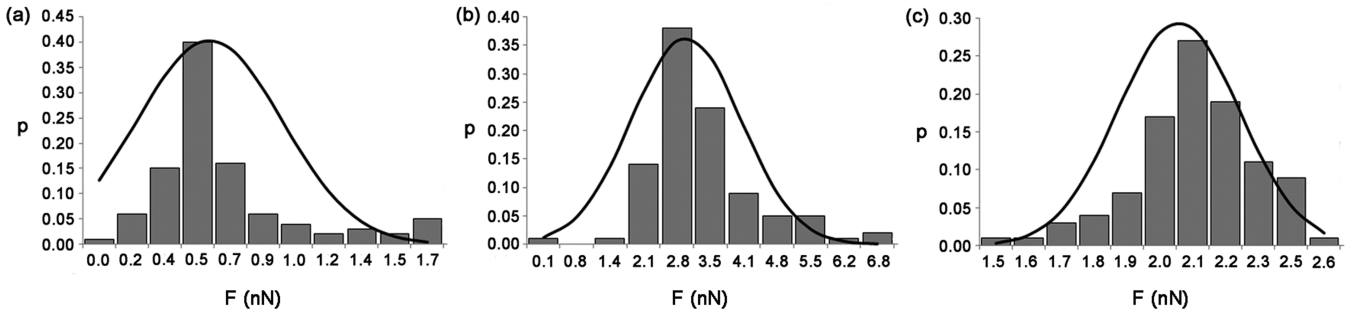

Figure 5. Comparison of adhesion force distributions for matrices: (a) NIF, (b) PU-MIF$_1$, and (c) PU-MIF$_2$ measured using the cell-probe ATCC 33003; p is the probability of the adhesion points presented within the scanned area on the polymer surface. The p value was calculated by being normalized to the total number of recorded force curves, N = 100.

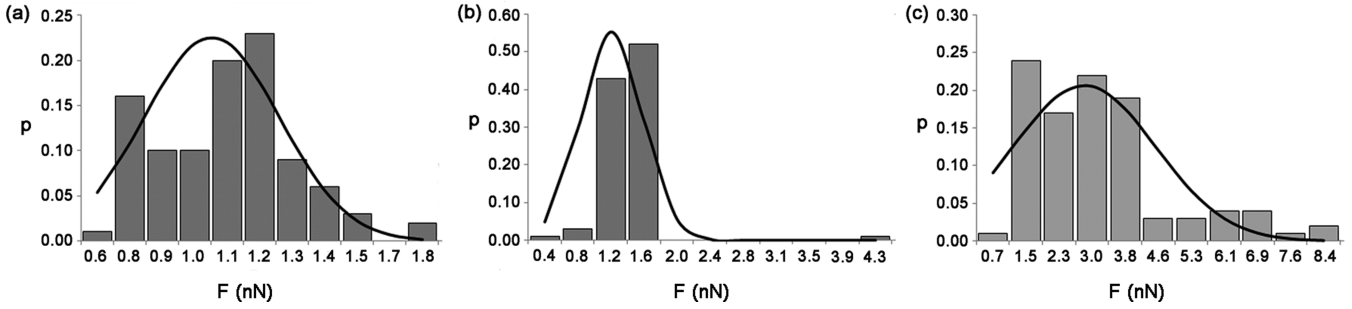

Figure 6. Comparison of adhesion force distributions for matrices: (a) NIF, (b) PU-MIF$_1$, and (c) PU-MIF$_2$ measured using the cell-probe ATCC 49242; p is the probability of the adhesion points presented within the scanned area on the polymer surface. The p value was calculated by being normalized to the total number of recorded force curves, N = 100.

even after 4 h; Figure 2a). To clearly demonstrate the change of imprinted sites, we collected SEM images of PU-MIFs after 4.0 h of water adsorption. As shown in Figure 2b,c, the sizes of imprinted sites were accorded with that of the original PU-MIF$_1$ and PU-MIF$_2$ (Figure 1b,c). These results indicated that imprinted sites on the surface of PU-MIFs remained to be intact and effective throughout the experiments. In addition, to verify the shelf life of PU-MIFs, PU-MIF$_1$ prepared at different time was viewed by SEM (Figure S3 in Supporting Information). And even up to 6 months, the shape of cavities remained intact.

In view of the application purpose, excellent biocompatibility of PU-MIFs for microorganism was highly demanded. To enhance the biocompatibility, here, PEG and CO were adopted to prepare PU-MIFs due to their superior biocompatibilities.[22] As a result of the clear definiteness in size and shape of methanotroph type strains, light microscopy was used to trace the cell growth. As shown in Figure 3, when cultured with corresponding PU-MIF, there were no distinct changes in the appearance of cells for either ATCC 33003 or ATCC 49242, suggesting the ideal biocompatibility of polymers. Besides, from Figure 3a,b, we could find that when cultured with PU-MIF$_1$, the growth of ATCC 33003 was accelerated. While for ATCC 49242 categorized to type II methanotroph, it was very easy to culture, and no such phenomenon was observed. This further demonstrated that the excellent biocompatibility of as-prepared material could not only provide a solid support for cell adhesion, but also offered a favorable matrix for cell differentiation and growth.[23]

3.2. Capture of Methanotroph Type Strains. To validate the ability of PU-MIFs on methanotroph enrichment, a confocal laser scanning microscope was used to observe the stained methanotroph type strains captured on PU-MIFs. ATCC 33003 and ATCC 49242 were stained with CellTracker Green CMFDA and CellTracker Orange CMTMR, respectively. As shown in Figure 4 (left panels), after incubating with stained ATCC 33003 or ATCC 49242, there was essentially no fluorescence observed on NIF, suggesting that NIF could not capture stained methanotrophs due to the absence of imprinted sites. While immersed into stained ATCC 33003 and ATCC 49242, many fluorescent dots were found on PU-MIF$_1$ and PU-MIF$_2$ (Figure 4a,b, middle panels). These results indicated that the PU-MIFs could easily capture its cognate methanotrophs. From the right panel of Figure 4a, we could find that there were some fluorescent dots detected as well, implying the few stained ATCC 33003 was also captured by noncognate PU-MIF$_2$. This was because (1) both ATCC 49242 and ATCC 33003 belong to a methanotroph, thus the chemical groups of lipopolysaccharide in the cell surface could be similar, and (2) because the size of ATCC 49242 was larger than that of ATCC 33003, the cavities created by the removal of ATCC 49242 (PU-MIF$_2$) were spacious enough to hold ATCC 33003. These results revealed that the PU-MIFs fabricated using the above method could selectively capture methanotroph type strains. And both chemical recognition sites and imprinted cavities on the PU-MIFs played key role in methanotroph capture.

3.3. Measurement of Affinity between Methanotroph and PU-MIFs. To probe the adhesion force between methanotroph and PU-MIFs, the AFM force spectroscopy was used in our experiments. ATCC 33003 and ATCC 49242 were immobilized onto the salinized Si_3N_4 tips respectively via hydrogen bond interaction arising from the hydroxyl groups on the surface of methanotroph and amino groups of the salinized Si_3N_4 tips.

Figure 5 showed the final distributions of the adhesive force needed to detach the cell-probe ATCC 33003 from the surface

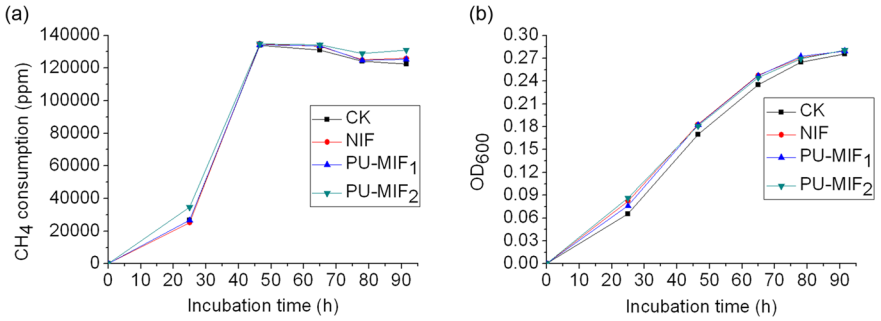

Figure 7. Plots of (a) CH_4 consumption and (b) OD_{600} of bacterial mixture obtained from paddy soil cultured with or without PU-MIFs or NIF. CK represents the sample without PU-MIFs and NIF. The average of three replicates was used for plotting.

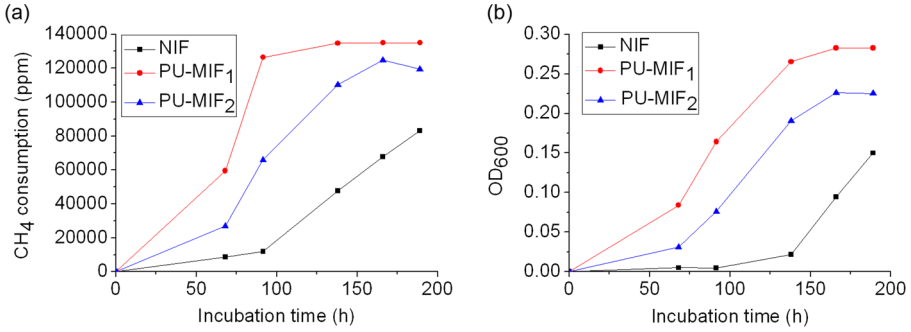

Figure 8. Recultivation of cells captured by PU-MIFs or NIF from microorganism mixture enriched from paddy soil. (a) CH_4 consumption of recultures cells solution; (b) OD_{600} of recultured cells solution. The average of three replicates was used for plotting.

of NIF, PU-MIF_1, and PU-MIF_2. Gauss function was fitted to determine the most probable detachment force. The adhesion force of ATCC 33003 to NIF (0.53 ± 0.44 nN; the error represents the half width at the half-maximum) surface was significantly lower than the adhesion forces to PU-MIF_1 (2.79 ± 1.29 nN) and PU-MIF_2 (2.13 ± 0.24 nN), suggesting the higher adhesion force was attributed to the imprinted cavities. And for PU-MIF_1, the highest adhesion force was obtained, implying that the affinity between the ATCC 33003 and PU-MIF_1 was strongest. This was because the imprinted cavities in PU-MIF_1 were formed by the removal of ATCC 33003, and so, the size, shape, and chemical recognition sites of the imprinted cavities matched to ATCC 33003 cells. Besides, force histograms showed that the adhesion force of ATCC 33003 to PU-MIF_2 was much higher than that to NIF (Figure 5); these results correspond to the results in Figure 4a. All of the above results confirmed that both the imprinted cavities and chemical recognition sites played a key role in methanotroph capture.

To further verify the selective recognition of the PU-MIFs, we used cell-probe ATCC 49242 to measure the adhesion force to different polymer matrices. Figure 6 presented the final distributions of the adhesion force used to detach the cell-probe ATCC 49242 from the surface of NIF, PU-MIF_1, and PU-MIF_2. And the adhesion force of ATCC 49242 to PU-MIF_2 (3.02 ± 1.95 nN) was significantly higher than that to PU-MIF_1 and NIF, suggesting that the affinity between the ATCC 49242 and PU-MIF_2 was strongest. Interestingly, the adhesion force of ATCC 49242 to PU-MIF_1 (1.19 ± 0.42 nN) surface was similar to that to NIF (1.09 ± 0.27 nN), implying that the imprinted sites on PU-MIF_1 produced by ATCC 33003 did not involve in adsorption process of ATCC 49242 to PU-MIF_2. This was because that the imprinted cavities on PU-MIF_1 were smaller in size than ATCC 49242, thus when the cell-probe ATCC 49242 approached the surface of PU-MIF_1, hydrogen bond interaction could only occur on the surface of PU-MIF_1 as NIF did. This also echoes the results shown in Figure 4b, where no stained cells were found on either NIF or PU-MIF_2, yet many stained cells were found on PU-MIF_1. These results not only confirmed the importance of matching imprinted sites to its cognate cells, but also certified the good selectivity of PU-MIFs for methanotroph recognition.

3.4. Application of PU-MIFs in Methanotroph Isolation from Rice Paddies. To further certify the probability of PU-MIF's application in real sample, we selected the microorganism mixture extracted from paddy soil as a research sample. The CH_4 consumption and OD_{600} were used as two main criteria for determining the growth of methanotrophs in samples. From Figure 7a, comparing to control, we could find that the CH_4 consumption amounts of the samples were basically consistent with PU-MIFs and NIF. These results further show that the PU-MIFs were harmless to methanotrophs. In addition, OD_{600} values of the samples added with PU-MIFs and NIF were slightly higher than that of the CK sample, implying that the polymer might promote cell growth.

In light of the above promising results, the PU-MIFs were used to isolate methanotrophs from the paddy soil samples. The CH_4 consumption and OD_{600} were selected to evaluate the growth situation of the cells captured by PU-MIFs as well. As shown in Figure 8, the CH_4 consumption and OD_{600} of the reculture solution of cells separated by NIF was far below that of PU-MIF_1 and PU-MIF_2 at the initial incubation time, suggesting that much more methanotrophs were captured due to the presence of abundant imprinted sites on PU-MIF_1 and PU-MIF_2. These results demonstrated that the PU-MIFs synthesized using methanotroph type stains as template could selectively enrich methanotrophs from paddy soil. Besides, in a very short time (0.5 h), the PU-MIFs could capture

dx.doi.org/10.1021/am506223k | ACS Appl. Mater. Interfaces 2014, 6, 20550−20556

methanotroph cells from paddy soil efficiently. Therefore, the application of PU-MIFs greatly shortened the experimental period of methanotroph screening from real samples. As shown in Figure 8, both the CH_4 consumption and OD_{600} of all samples increased with incubation time. This was caused by the proliferation of other microorganisms ascribing to the nonspecific adsorption. Thus, although the PU-MIFs could isolate methanotrophs from paddy soil, the selectivity and specificity needed to be further improved.

4. CONCLUSIONS

We have demonstrated the use of PU-MIFs for methanotroph isolation from rice paddy soil for the first time. This kind of PU-MIF has excellent biocompatibility and selectivity for template cell. By modifying the AFM probe, the adhesion force between methanotroph and polymer was measured, and results elucidated the reason that PU-MIFs could selectively enrich cells. When using this protocol in the isolation of methanotroph from a real sample, PU-MIFs can dramatically shorten the enrichment time. The PU-MIFs not only can be applied in the isolation and recognition of methanotroph from sample but also have potential in producing sensing elements for environmental monitoring, medical diagnostics, and the identification or quantification of harmful microorganisms in food.

■ ASSOCIATED CONTENT

Supporting Information

SEM images of PU-MIFs without template removal; AFM images of NIF, PU-MIF_1, and PU-MIF_2; SEM images of PU-MIF_1 prepared at different time. This material is available free of charge via the Internet at http://pubs.acs.org.

■ AUTHOR INFORMATION

Corresponding Author

*Tel.: 861062731255 E-mail: renxueqin@cau.edu.cn.

Notes

The authors declare no competing financial interest.

■ ACKNOWLEDGMENTS

We thank Weiqi Wang of The State Key Laboratory of Tribology, Tsinghua University, for supplying technical support in AFM experiments. This work was supported by the Chinese National Scientific Foundation (Grant Nos. 21375146 and 41130527).

■ REFERENCES

(1) Nisbet, E. G.; Dlugokencky, E. J.; Bousquet, P. Methane on the Rise—Again. *Science* **2014**, *343*, 493−495.

(2) Kirschke, S.; et al. Three Decades of Global Methane Sources and Sinks. *Nat. Geosci.* **2013**, *6*, 813−823.

(3) Bodelier, P. L. E.; Steenbergh, A. K. Interactions between Methane and the Nitrogen Cycle in Light of Climate Change. *Curr. Opin. Environ. Sustainability* **2014**, *9*−*10*, 26−36.

(4) Mer, J. L.; Roger, P. Production, Oxidation, Emission and Consumption of Methane by Soils: A Review. *Eur. J. Soil Biol.* **2001**, *37*, 25−50.

(5) Hanson, R. S.; Hanson, T. E. Methanotrophic Bacteria. *Microbiol. Rev.* **1996**, *60*, 439−471.

(6) Eersels, K.; et al. Selective Identification of Macrophages and Cancer Cells Based on Thermal Transport through Surface-Imprinted Polymer Layers. *ACS Appl. Mater. Interfaces* **2013**, *5*, 7258−7267.

(7) Xu, L.; Hu, Y. F.; Shen, F.; Li, Q. S.; Ren, X. Q. Specific Recognition of Tyrosine-Phosphorylated Peptides by Epitope Imprinting of Phenylphosphonic Acid. *J. Chromatogr., A* **2013**, *1293*, 85−91.

(8) Li, D. Y.; He, X. W.; Chen, Y.; Li, W. Y.; Zhang, Y. K. Novel Hybrid Structure Silica/CdTe/Molecularly Imprinted Polymer: Synthesis, Specific Recognition, and Quantitative Fluorescence Detection of Bovine Hemoglobin. *ACS Appl. Mater. Interfaces* **2013**, *5*, 12609−12616.

(9) He, Y. H.; Huang, Y. Y.; Jin, Y. L.; Liu, X. J.; Liu, G. Q.; Zhao, R. Well-Defined Nanostructured Surface-Imprinted Polymers for Highly Selective Magnetic Separation of Fluoroquinolones in Human Urine. *ACS Appl. Mater. Interfaces* **2014**, *6*, 9634−9642.

(10) Hayden, O.; Dickert, F. L. Selective Microorganism Detection with Cell Surface Imprinted Polymers. *Adv. Mater.* **2001**, *13*, 1480−1483.

(11) Dickert, F. L.; Hayden, O. Bioimprinting of Polymers and Sol−Gel Phases. Selective Detection of Yeasts with Imprinted Polymers. *Anal. Chem.* **2002**, *74*, 1302−1306.

(12) Seidler, K.; Lieberzeit, P. A.; Dickert, F. L. Application of Yeast Imprinting in Biotechnology and Process Control. *Analyst* **2009**, *134*, 361−366.

(13) Hachulka, K.; Lekka, M.; Okrajni, J.; Ambroziak, W.; Wandelt, B. Polymeric Sensing System Molecularly Imprinted towards Enhanced Adhesion of Saccharomyces Cerevisiae. *Biosens. Bioelectron.* **2010**, *26*, 50−54.

(14) Schirhagl, R.; Hall, E. W.; Fuereder, I.; Zare, R. N. Separation of Bacteria with Imprinted Polymeric Films. *Analyst* **2012**, *137*, 1495−1499.

(15) Ren, K. N.; Banaei, N.; Zare, R. N. Sorting Inactivated Cells Using Cell-Imprinted Polymer Thin Films. *ACS Nano* **2013**, *7*, 6031−6036.

(16) Panos, M.; Sen, T. Z.; Ahunbay, M. G. Molecular Simulation of Fibronectin Adsorption onto Polyurethane Surfaces. *Langmuir* **2012**, *28*, 12619−12628.

(17) Nohra, B.; Candy, L.; Blanco, J. F.; Guerin, C.; Raoul, Y.; Mouloungui, Z. From Petrochemical Polyurethanes to Biobased Polyhydroxyurethanes. *Macromolecules* **2013**, *46*, 3771−3792.

(18) Blanchette, C. D.; Loui, A.; Ratto, T. V. In *Handbook of Molecular Force Spectroscopy*; Noy, A., Eds.; Springer: New York, 2008; Chapter 7, pp 185−204.

(19) Beaussart, A.; El-Kirat-Chatel, S.; Sullan, R. M. A; Alsteens, D.; Herman, P.; Derclaye, S.; Dufrene, Y. F. Quantifying the Forces Guiding Microbial Cell Adhesion Using Single-Cell Force Spectroscopy. *Nat. Protoc.* **2014**, *9*, 1049−1055.

(20) Bourne, D. G.; Holmes, A. J.; Iversen, N.; Murrell, J. C. Fluorescent Oligonucleotide rDNA Probes for Specific Detection of Methane Oxidising Bacteria. *FEMS Microbiol. Ecol.* **2000**, *31*, 29−38.

(21) Sirkecioglu, A.; Mutlu, H. B.; Citak, C.; Koc, A.; Guner, F. S. Physical and Surface Properties of Polyurethane Hydrogels in Relation with Their Chemical Structure. *Polym. Eng. Sci.* **2014**, *54*, 1182−1191.

(22) Miao, S.; Wang, P.; Su, Z. G.; Zhang, S. P. Vegetable-Oil-based Polymers as Future Polymeric Biomaterials. *Acta Biomater.* **2014**, *10*, 1692−1704.

(23) DePorter, S. M.; Lui, I.; McNaughton, B. R. Programmed Cell Adhesion and Growth on Cell-Imprinted Polyacrylamide Hydrogels. *Soft Matter* **2012**, *8*, 10403−10408.